

## **CORROSION PERFORMANCE OF EPOXY-COATED REBAR IN FLORIDA KEYS BRIDGES**

Alberto A. Sagüés  
Department of Civil and Environmental Engineering  
University of South Florida  
Tampa, Florida 33620

Rodney G. Powers and Richard Kessler  
Materials Office  
Florida Department of Transportation  
2006 N.E. Waldo Rd.  
Gainesville, Florida 32609

### **ABSTRACT**

Severe corrosion of epoxy coated rebar in the substructure of 5 major marine bridges in the Florida Keys was detected after only a few years of construction. Corrosion occurred underneath the coating and was preceded by loss of adherence between the steel and the coating. Damage surveys of the bridges, which were built around 1980, were conducted from 1986 to 2000. Corrosion resulted in delaminated areas (spalls) typically about 0.3 m<sup>2</sup> each. After Initial detection, damage has been steadily accumulating at a rate of approximately 0.1 spall per bridge pier (bent) per year. An initiation-propagation model for corrosion development reproduced the observed trends. The exploratory model assumes distribution of chloride diffusivity, rebar cover, chloride surface concentration, and propagation time. Interpretation of the results suggests that much of the early damage stemmed from rebar with high levels of coating distress, and that damage development depends mainly on the propagation stage of corrosion.

Keywords: epoxy, rebar, concrete, Florida Keys, corrosion, bridges

## INTRODUCTION

Epoxy-coated rebar (ECR) has been used in approximately 300 Florida bridges, principally in an attempt to control corrosion of the substructure in the splash-evaporation zone of marine bridges. Starting in 1986, severe corrosion of ECR began to be observed in five major bridges built between 1978 and 1983 along US 1 in the Florida Keys <sup>(1-3)</sup>. The development of corrosion damage has been recorded periodically. An update for the first 20 years of structural service life is presented here.

Table 1 lists the structures affected, nomenclature, and construction information. Three of the bridges (7MI, NIL and INK) were built with drilled shafts supporting columns with connecting struts. The LKY bridge had capped drilled shafts joined by a strut, and V-Piers rested on synthetic rubber pads placed on the caps. The CH5 bridge had drilled shafts with spread footers and precast, posttensioned box columns.

Unless indicated otherwise, the concrete used in the substructure was cast in place (CIP) and conforming to FDOT Class IV specifications at the time of construction. Those specifications established  $w/c < 0.41$ , cement content =  $388 \text{ Kg/m}^3$  ( $658 \text{ lb/yd}^3$ ), and 28-day strength  $> 23.5 \text{ MPa}$  ( $3,400 \text{ psi}$ ). The fine aggregate was sand and the coarse aggregate oolitic limestone. The cement type for each structure is indicated in Table 1. The specified maximum chloride content (acid soluble test) for concrete in these structures was  $0.24 \text{ kg/m}^3$  ( $0.4 \text{ lb/yd}^3$ ). The design clear rebar concrete cover for the substructure of these bridges was 76 mm (3 in). Substantial deviations from that value were often observed, especially in round columns when the rebar cage was not precisely centered. As a result, it was not uncommon to encounter concrete cover as little as 25 mm (1 in) on one side of the column and 125 mm (5 in) on the other side. Some instances of no cover were encountered.

Initial chloride content of the concrete in the bridges (from FDOT records) was small for NIL, LKY and CH5, but that it was considerably higher for 7MI ( $1.8 \text{ kg/m}^3$  ( $2.9 \text{ lb/yd}^3$ )) and INK ( $0.7 - 2.1 \text{ kg/m}^3$  ( $1.1 - 3.5 \text{ lb/yd}^3$ )). It has been speculated that the higher values reflected seawater contamination of the coarse aggregate.

The ECR had been manufactured and coated following ASTM 775 - 76 and ECR placement guidelines in place at the time of construction <sup>(1-2)</sup>. Those guidelines allowed a maximum of 2% unrepaired surface damage at rebar surface. The coating material and applicators for each bridge are listed in Table 1. Rebar sizes ranged from #3 (10 mm diameter) to # 8 (25 mm). Rebar tie wires, as revealed by direct examination, were bare steel.

Conventional patch repairs and corrosion control procedures were conducted at various times in selected bents (piers) of these bridges. The most notable protective procedure was installation starting in 1988 of sacrificial sprayed-zinc anodes <sup>(4)</sup> at LKY (38 bents by 1996 plus 30 bents by 1998), NIL (31 bents by 1996), and 7MI (148 bents by 1998). In some instances the anodes were supplemented by immersed bulk anodes <sup>(4)</sup>. Information being compiled at this time indicates substantial corrosion mitigation in the elements protected by this method. Other procedures included patching with concrete incorporating corrosion inhibiting admixtures, bar coatings, and proprietary cementitious repair mortars. The effect of these procedures is being evaluated.

Examination of the structures was conducted at various levels. A general visual examination, performed periodically, was made by an experienced crew travelling slowly by boat and examining the entire perimeter of each bent in the bridge. If evidence of cracking or other distress was observed, the substructure element was tested by sounding with a hammer for evidence and extent of internal delamination. An area of delaminated concrete thus detected was designated as a concrete spall. A delaminated area which extended from an area found to be spalled in a previous inspection was designated as a progressive spall. On selected bents, the delaminated concrete was removed to expose the ECR and directly determine the extent of corrosion. Chloride ion (acid soluble) concentration profile measurements were conducted on cores extracted from selected bents.

Table 2 lists the results of visual and sounding examinations performed between 1986 and 2000. The number of new spalls or progressive spalls observed on a bridge at a given inspection date was recorded. That number was then added to those observed in the previous inspections of the same bridge, and reported in Table 2 as the cumulative number of spalls to the listed date. Spalls that occurred in regions formerly repaired (either by conventional patching or otherwise) were considered a new spalls.



FIGURE 1 - Typical spall appearance (7MI)

Figure 1 shows the macroscopic morphology of corrosion of a typical spall, after removal of the concrete cover. Typical spalls affected a projected area of  $\sim 0.3 \text{ m}^2$  ( $\sim 3 \text{ sq.ft.}$ ) on the surface of the concrete. Although rust stains are present on the delaminated surface, much of

the epoxy coating is still visible on the rebar. Longitudinal cuts with a sharp knife permit easy peeling of the coating from the corroded regions, revealing extensive corrosion products underneath. Those internal corrosion products were generally solid, dark, magnetic and electronically conductive<sup>(5)</sup>. Occasionally, significant amounts of acidic liquid rich in chloride and iron were found as well<sup>(6,7)</sup>.

Sandblasting of the corroded region to remove the epoxy and corrosion products revealed that extensive metal loss had occurred, in the form of pits several mm long and deep. In some instances, corrosion-free steel tie wire was found in contact with corroding regions of the ECR.

The coating on rebar adjacent to and also away from the corroding region was found to be easy to peel after cutting with a knife, revealing bright or slightly darkened metal underneath. This disbondment without significant corrosion was found to be widespread in ECR after it was in service for a few years in Florida marine substructure conditions, even in the absence of chloride contamination of the concrete next to the rebar<sup>(8,9)</sup>. Examination of the underside of coatings from numerous ECR samples from Florida bridges did not reveal any correlation between this disbondment and the usual forms of surface contamination expected in the coating process<sup>(8,9)</sup>.

Chloride ion profiles indicated that extensive chloride penetration of the concrete had taken place in the splash zone of the structures affected. At the time of the first spall observations, chloride content at a depth of 50 mm to 76 mm in the splash zone of LKY, 7MI and NIL was between 8 kg/m<sup>3</sup> (14 pcy) and 14 kg/m<sup>3</sup> (24 pcy)<sup>(9)</sup>. Apparent chloride diffusion coefficients ( $D_{app}$ ) determined from the chloride profiles for the splash zone in those bridges ranged from  $\sim 10^{-8}$  cm<sup>2</sup>/sec ( $\sim 0.1$  in<sup>2</sup>/y) to as much as  $\sim 6 \cdot 10^{-7}$  cm<sup>2</sup>/sec ( $\sim 3$  in<sup>2</sup>/y)<sup>(9,11)</sup>. These high diffusivities agreed with concrete resistivity readings as low as  $\sim 1$  k $\Omega$  cm in the tidal region<sup>(9,10,12)</sup>.

## DISCUSSION

### Corrosion Mechanism

The corrosion mechanism of ECR in concrete has been discussed earlier<sup>(8)</sup> and a proposed scenario for the continuing development of corrosion at the Florida Keys bridges is summarized next. This scenario is consistent with the field observations and with the results of previous investigations<sup>(9)</sup>.

*Pre-service history:* ECR was produced according to the specifications existing at the time of the construction projects (Figure 2 A). The bars contained a small number of initial coating imperfections, as permitted by the acceptance criteria. The bars were cut, shaped and then shipped and fabricated as required. Shipping introduced additional surface damage; fabrication mechanically introduced some disbondment<sup>(3)</sup> (B). The bars were exposed to the construction yard environment for a time that may have ranged from days to over a year. Salt water (from sea spray) exposure at the yard created additional disbondment; further deterioration might have resulted from heating/cooling cycles, ultraviolet exposure and additional mechanical damage during handling (C). Rebar cage assembly procedures, positioning in concrete forms, as well as concrete pouring and vibration, created additional surface damage.

*Service-in-concrete history:* The ECR was exposed to a low (or, in two of the bridges, intermediate) chloride concrete environment for some time depending on the rate of chloride penetration. During that time the concrete pore solution interacted with the rebar coating, and penetrated between coating and metal in regions where disbondment had taken place during pre-service. Exposure to the low or intermediate chloride content concrete aggravated coating delamination (D).

*In summary,* the corrosion may be viewed as resulting from the presence of allowable (at the time of manufacturing) production imperfections which were then aggravated by fabrication, handling, and a severe construction yard environment. This was followed by placing the rebars in moist, warm, eventually high chloride-level substructure service which was conducive to severe corrosion, aggravated by extended macrocell formation.

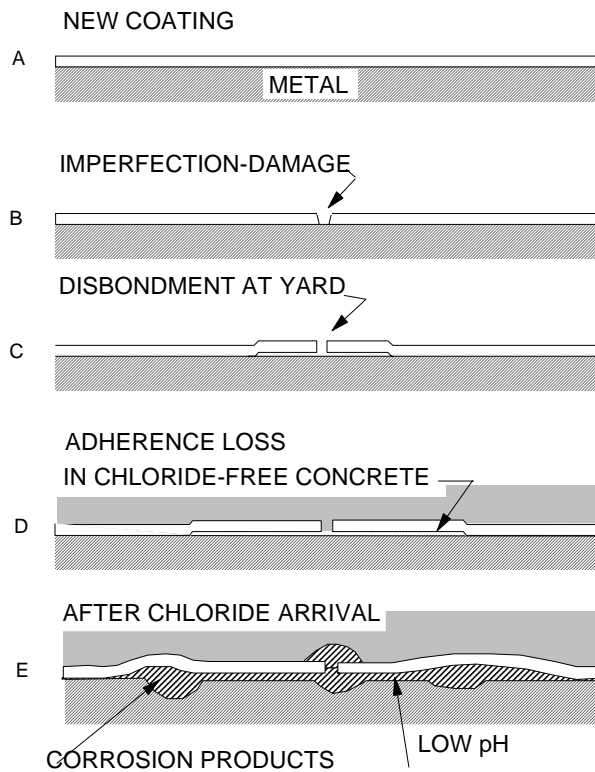


FIGURE 2 - Schematic corrosion sequence <sup>(3,9)</sup>. Steps D and E overlap for concrete with high initial chloride content.

### Corrosion Progression

To compare the progression of corrosion in bridges of different lengths, the data in Table 2 were normalized by dividing the number of spalls by the number of bents in each bridge. The resulting damage functions (spalls per bent as function of time) are plotted in Figure 3. The corrosion damage after nearly 20 years of service is conspicuous (more than one spall per bent) and affects a significant fraction of the area of the splash zone of each bridge (the concrete

surface area on the splash zone of a typical bent is  $\sim 20 \text{ m}^2$  while a typical spall affects  $\sim 0.3 \text{ m}^2$ ). Damage is likely to have been worse without the application of protective anodes. Except for an offset toward shorter times for NIL, the functions are remarkably similar to each other. The damage at present appears to increase approximately linearly with time. If those trends were to continue, the total extent of damage would roughly double over the next 20 years of service. As repairs in marine substructure are very costly, corrosion would place a continuing and heavy repair and maintenance burden during the service life of these structures.

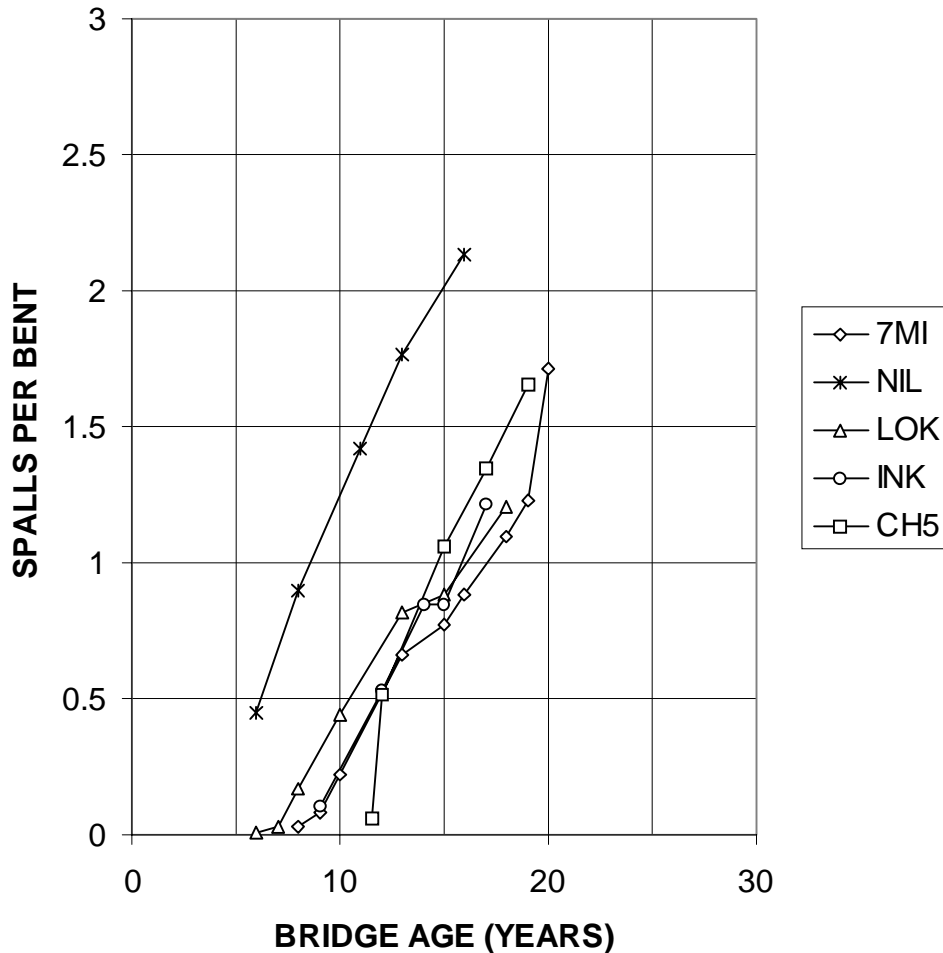


FIGURE 3. Progression of corrosion as function of time. Data from Table 2 were normalized by dividing by the number of bents in each bridge.

### Corrosion Projections

Research is ongoing on a model to try to explain the observed damage progression, based on the present understanding of corrosion in concrete, to better substantiate projections for future performance in these bridges. The impact of corrosion control procedures in the observed damage functions will be ignored for the moment. The simplest corrosion forecasting involves a two-step approach<sup>(10,13)</sup>. In the first step (initiation), the chloride ion concentration at the surface of the ECR is considered to be below the critical threshold for appearance of active corrosion of

the steel. The concentration, however, is increasing constantly because of chloride transport through the concrete cover. The initiation period ends when the chloride concentration at the rebar surface reaches the critical threshold value  $C_T$ . During the propagation period corrosion products accumulate. The propagation period ends with the development of concrete cover spalls or concrete cracks.

The length of the initiation period can be evaluated by making the simplifying assumptions that chloride ions move only by diffusion, and that the concentration of chloride ions at the concrete surface reaches a value (constant in time) shortly after the substructure member is placed in service. The one-dimensional solution to the diffusion equation is used to calculate the time  $t_i$  needed for chloride buildup at the rebar surface to reach an assumed critical threshold value  $C_T$ . The length  $t_p$  for the propagation period can be estimated as indicated later.

Under the above assumptions the damage function for a structural element with uniform concrete cover, concrete and rebar properties, and exposure conditions, would take the form of a step function: no observable damage before  $t_i + t_p$ , and complete spalling of the element afterwards. However, the appearance of the functions in Figure 3 indicates that the development of damage was gradual instead. This behavior may be envisioned as resulting from the superposition of numerous individual step functions corresponding to the end of the propagation stage of different portions of the structure each with its own values of  $C_s$ , concrete cover  $x$ ,  $D_{app}$ ,  $C_T$ , and  $t_p$ . Mathematical treatments to simulate that situation have been reported, initially assuming only variability in  $x$  <sup>(14)</sup>, and later in several of the parameters <sup>(11,15)</sup>. That approach was used here as well.

An accurate prediction of damage development is not possible at this time because precise knowledge of the parameters relevant for damage development is not available. However, some insight on the factors responsible for the corrosion progression may be gained by assuming parameter values and variabilities typical of these structures.  $C_s$  is known to reach  $\sim 14 \text{ kg/m}^3$  <sup>(9)</sup> at the bottom of the splash evaporation zone and decrease with increasing elevation. The design value of  $x$  (76 mm), and the range of variation of  $x$  (0 to 160 mm), are known from specifications and can be estimated from field observations respectively. Typical  $D_{app}$  values are on the order of  $10^{-11} \text{ m}^2/\text{sec}$ , as indicated by analyses of chloride concentration profiles extracted from some of the bridges <sup>(9)</sup>. Laboratory observations suggest that under simple conditions  $C_T$  for ECR is on the order of the value for plain steel bar <sup>(9)</sup>, which may in turn be estimated as being proportional to the cement content (CF) of the concrete,  $C_T \sim 0.004 \text{ CF}$  <sup>(16)</sup>. The value of  $t_p$  is expected to depend mostly on  $x$  and on the corrosion rate of the rebar. There is growing evidence that, for a given corrosion rate and rebar size,  $t_p$  of conventional rebar (and likely also for ECR) is directly proportional to  $x$  <sup>(17)</sup>. For a particular value of  $x$  and rebar size,  $t_p$  should be longer as the rebar corrosion rate is smaller <sup>(17)</sup>. The corrosion rate is strongly influenced by the condition of the coating <sup>(18,19)</sup>; ECR with substantial coating distress should corrode faster than in the absence of imperfections. For modeling purposes,  $t_p$  can then be expressed as  $t_p = k x$ , where  $k$  is a parameter that becomes smaller as the extent of ECR coating distress increases.

The present system was tentatively modeled using the procedure of Sagüés et al <sup>(15)</sup> by assuming that the observed damage functions resulted from normal distributions, truncated as appropriate, in the values of  $x$ ,  $D_{app}$  and  $C_s$ . In addition variability in  $t_p$  (through the parameter  $k$ ) was introduced based on the above discussion, and because it produced plausible results when used together with the value of  $C_T$  indicated earlier. As in Ref.[15], the surface of a generic

bridge bent was divided into equal area elements each having an individual set of parameters  $x$ ,  $D_{app}$  and  $C_s$  as well as  $k$ . The damage from individual elements was tallied as time progressed to obtain the total damage function.

Figure 4 shows an example of a model calculation using as input the parameters and variabilities listed in Table 3, based on the typical values indicated earlier. The calculations assumed initially chloride-free concrete. The assignment of  $k$  values over the rebar assembly, which was treated for simplicity as a discrete distribution, assumed that only a small fraction (2%) of the rebar assembly was responsible for the earliest observations of damage. That fraction had a low value of  $k$  (0.14 y/mm, which results in  $t_p=7$  years when  $x=50$  mm) and consequently was responsible for the very first failures projected. Increasingly large fractions of the assembly were assumed to have correspondingly larger propagation times. This approach is based on the expectation that rebar segments with a high incidence of coating distress are likely to have the highest corrosion rates and therefore the shortest  $t_p$  values. The chosen distribution for  $k$  then effectively states that there was a small fraction of the rebar with severe coating distress, and proportionally less distress on increasing fractions of the assembly. The effect of these assumptions is apparent in the dashed lines of Figure 4, which show the contribution to the total damage from each of the distress fractions assumed.

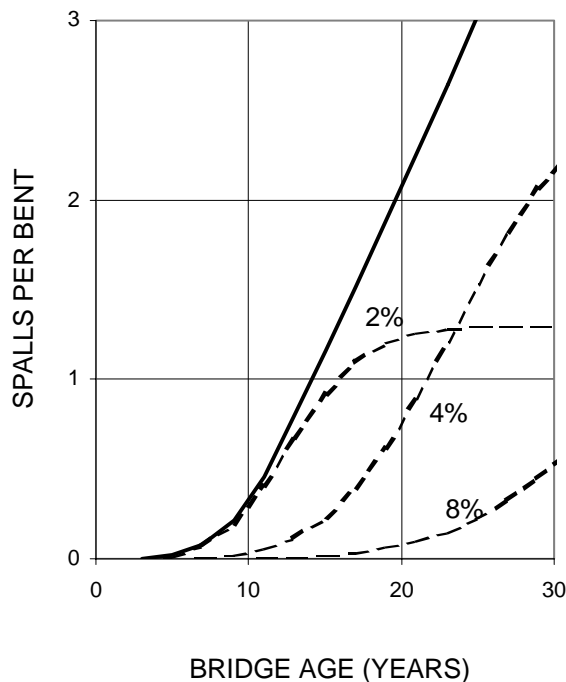


Figure 4 - Illustration of a projected damage function generally replicating the features and values of the behavior in Figure 3. The solid line corresponds to the total damage projection. The dashed lines correspond to the partial damage from each of the rebar assembly fractions considered: 2% of the rebar with  $k=0.14$  y/mm; 4% with  $k=0.28$  y/mm and 8% with  $k=0.56$  y/mm. Adding up the partial damages yields the total damage.

The choice of input parameters used yielded a projected damage evolution for the first 20 years that was consistent with the observed behavior in Figure 3. The projection reasonably

reproduced the duration of the initial period with minimal damage, and the subsequent steady rise at a rate of  $\sim 0.1$  spall/bent/year observed in the bridges. Sensitivity tests showed that the damage projection was only modestly influenced by changes in the distribution of  $D_{app}$  or  $C_s$ , or by variations in  $C_T$ . This behavior is a consequence of the severe exposure regime assumed, which causes the corrosion threshold to be reached at much of the rebar surface very early in the simulation. A similar circumstance may account in the actual structures for the little differentiation (Figure 3) between the trends in 7MI and INK, which had initial chloride contamination, and that of the other bridges. Thus the projected behavior was determined mainly by the corrosion propagation phase, which depended strongly on the  $k$  values and cover distribution assumed. It was felt that the chosen value for the variability of  $x$  (described by the parameter  $scc$  in Table 3) was reasonably representative as it allowed for  $\sim 10\%$  of the cover to be less than 5 cm, reflecting several observations of low cover during inspection of the first recorded spalls. The  $k$  distribution chosen for Table 3 was only a working example. However, ranging calculations confirmed that reasonable fit to observed behavior could be obtained only if the percentage of the assembly assigned low  $k$  values (yielding  $tp$  values of only a few years) was quite small.

While exploratory in nature, the model projections provide some insight as to possible future behavior if the actual systems. As shown in Figure 4, as time progresses the projected damage results from fractions with increasingly greater  $k$ . Whether future damage will continue along the present trend depends, in this scheme, on the extent of coating distress on the rest of the rebar assembly. If the remaining rebar coating were in very good condition, damage would continue for some time at the present rate and then saturate at some intermediate level. In the case of the values assumed for Table 3, there was no  $k$  value assigned beyond the first 14% of the rebar assembly, and damage would saturate at  $\sim 9$  spalls per bent. If the condition of the remaining rebar were poor or marginal, damage progression would not saturate soon, and could even accelerate.

The interpretation and model described above involve numerous assumptions and simplifications. Notable among the many issues not addressed are alternative  $C_T$  regimes as reported elsewhere<sup>(11)</sup>, including possible higher  $C_T$  due to coupling with nearby anodic regions<sup>(20)</sup> which could dramatically alter the damage projection. Comparison with the behavior of similar systems with uncoated rebar is also needed. Alternative models are addressing those issues, as well as incorporating the effect of corrosion protection measures such as sacrificial sprayed-zinc anodes. The analysis presented here underscores the importance of continuing characterization and damage development monitoring in these structures, to improve understanding of the critical factors responsible for their deterioration.

## CONCLUSIONS

1. Damage from corrosion of ECR has continued to develop steadily in the substructure of 5 major Florida Keys bridges. Since the first indications of corrosion  $\sim 6$  y after construction, damage increased at a rate of  $\sim 0.1$  spall per bent per year until the present  $\sim 20$  y age of the structures, with no indication of slowdown.
2. Chloride penetration in concrete was very fast in the exposure conditions of the bridges. The results and model calculations suggest that the propagation stage plays a strong role in the rate of development of corrosion.

3. Exploratory model calculations suggest that much of the early corrosion damage stemmed from a relatively small fraction of the rebar, with high levels of coating distress. Later corrosion development is projected to be controlled by rebar with lesser coating distress.

## ACKNOWLEDGMENT

This work was supported by the Florida Department of Transportation. The findings and conclusions expressed here are those of the authors and not necessarily those of the Florida Department of Transportation.

## BIBLIOGRAPHY

1. Kessler, R. and Powers, R. Interim Report, Corrosion Evaluation of Substructure, Long Key Bridge, Corrosion Report No. 87-9A, Materials Office, Florida Department of Transportation, Gainesville, 1987.
2. Powers, R. Corrosion of Epoxy Coated Rebar, Keys Segmental Bridges, Corrosion Report No. 88-8A, Florida Dept. of Transportation, Gainesville, Florida, 1987.
3. Sagüés, A., Powers, R. and Kessler, R., "Corrosion Processes and Field Performance of Epoxy Coated Reinforcing Steel in Marine Substructures", Paper No. 299, Corrosion/94, NACE International, Houston, 1994.
4. Kessler, R. and Powers, R., "Zinc Metallizing for Galvanic Cathodic Protection of Steel reinforced Concrete in a Marine Environment", Paper No. 324, Corrosion/90, NACE International, Houston, 1990.
5. Sagüés, A., Powers, R., Zayed, A., "Marine Environment Corrosion of Epoxy-Coated Reinforcing Steel", in Corrosion of Reinforcement in Concrete, C. Page, K.Treadaway and P. Bamforth, Eds., pp.539-549, Elsevier Appl. Sci., London-New York, 1990.
6. Sagüés, A. and Powers, R., "Effect of Concrete Environment on the Corrosion Performance of Epoxy-Coated Reinforcing Steel", Paper No. 311, Corrosion/90, NACE International, Houston, 1990.
7. Sagüés, A. , Perez-Duran. H. and Powers, R., Corrosion, Vol 47, p.884, 1991.
8. Sagüés, A. and Powers, R. "Coating Disbondment in Epoxy-Coated Reinforcing Steel in Concrete - Field Observations", Paper No. 325, Corrosion/96, NACE International, Houston, 1996.
9. Sagüés, A. "Corrosion of Epoxy-Coated Rebar in Florida Bridges", Final Report to Florida DOT, WPI No. 0510603, Florida Department of Transportation, Tallahassee, FL, May, 1994.

10. Berke, N.S. and Hicks, M.C., "Estimating the Life Cycle of Reinforced Concrete Decks and Marine Piles using Laboratory Diffusion and Corrosion Data", p. 207 in Corrosion Forms and Control for Infrastructure, ASTM STP 1137, Victor Chaker, Ed., ASTM, Philadelphia, 1992.
11. Hartt, W., Lee, S.K. and Costa, J., "Condition Assessment and Deterioration Rate Projection for Chloride Contaminated Concrete Structures" p.82 in Repair and Rehabilitation of Reinforced Concrete Structures: The State of the Art, W.P. Silva-Araya, O. T. de Rincon and L. Pumarada O'Neill, Eds., ASCE, Reston, VA, 1998.
12. Andrade, C., Alonso, C. and Goni, S., "Possibilities for Electrical Resistivity to Universally Characterise Mass Transport Processes in Concrete", p.1639, in Concrete 2000, Vol 2., R.K. Dhir and M.R. Jones, Eds., E. & F.N. Spon, London, 1993.
13. Tuutti, K., Corrosion of Steel in Concrete, Swedish Cement and Concrete Research Institute, 1982.
14. Weyers, R.E. et al, "Concrete Bridge Protection, Repair and Rehabilitation Relative to Reinforcement Corrosion, a Methods Application Manual", Strategic Highway Research Program, National Research Council, Washington, D.C., 1993.
15. Sagüés, A.A., Scannel, W. and Soh, F.W., "Development of a Deterioration Model to Project Future Concrete Reinforcement Corrosion in a Dual Marine Bridge", in Proc. International Conference on Corrosion and Rehabilitation of Reinforced Concrete Structures, Orlando, FL, Dec. 7-11, 1998, CD ROM Publication No. FHWA-SA-99-014, Federal Highway Administration, 1998.
16. Bentur, A., Diamond, S. and Berke, N., Steel Corrosion in Concrete, E&FN Spon, New York, 1997.
17. "Concrete Cover Cracking with Localized Corrosion of the Reinforcing Steel", A.A. Torres-Acosta and A.A. Sagüés, p. 591 in Proc. of the Fifth CANMET/ACI Int. Conf. on Durability of Concrete, SP-192, V.M Malhotra, Ed., American Concrete Institute, Farmington Hills, Mich., U.S.A., 2000.
18. Clear, K.C., "Effectiveness of Epoxy-Coated Reinforcing Steel", Concrete International, p. 58, Vol. 14, May 1992.
19. McDonald, D.B, Pfeifer, D.W. and Sherman, M.R, "Corrosion Evaluation of Epoxy-Coated, Metallic-Clad and Solid Metallic Reinforcing Bars in Concrete", Report No. FHWA-RD-98-153, Nat. Tech. Info. Service, Springfield, VA, 1998.
20. Sagüés, A.A. and Kranc, S.C. "Model for a Quantitative Corrosion Damage Function for Reinforced Concrete Marine Substructure" in Rehabilitation of Corrosion Damaged Infrastructure, p.268, Proceedings, Symposium 3, 3rd. NACE Latin-American Region Corrosion Congress, P.Castro, O.Troconis and C. Andrade, Eds., ISBN 970-92095-0-7, NACE International, Houston, 1998.

TABLE 1.  
BRIDGE INFORMATION

BRIDGE	7 MILE (7MI)	NILES CHANNEL (NIL)	LONG KEY (LKY)	INDIAN KEY (INK)	CHANNEL #5 (CH5)
FDOT Bridge Number	900020	900117	900094	900095	900098
Year Built	1980	1982	1980	1981	1981
Number of Bents	264	38	102	19	35
ECR Source	Florida Steel	Bethlehem Steel	Florida Steel	Bethlehem Steel	Bethlehem Steel
Epoxy Coating Powder	Scotchkote 213	Scotchkote 213	Scotchkote 213  Hysol	Scotchkote 213	Scotchkote 213
Coating Applicator	Rezcom (Drilled Shafts)  Santa Fe	Lane Metals  MCP	Rezcom	MCP  Lane Metals	MCP
Cement Type	II	II and III	I and III	II	III
Initial Concrete Cl <sup>-</sup> Content (kg/m <sup>3</sup> )	1.7	0.15	0.15	0.65 - 2.1	0.15

TABLE 2.  
CUMULATIVE NUMBER OF SPALLS OBSERVED TO DATE OF INSPECTION

BRIDGE	7 MILE (7MI)	NILES CHANNEL (NIL)	LONG KEY (LKY)	INDIAN KEY (INK)	CHANNEL #5 (CH5)
Year Built	1980	1982	1980	1981	1981
Number of Bents	264	38	102	19	35
INSPECTION DATE			CUMULATIVE NUMBER OF SPALLS		
1986			1		
1987			3		
1988	8	17	17		
1989	22				
1990	58	34	45	2	
1993 (1st)					2
1993 (2nd)	175	54	83	10	18
1995	204	67	90	16	
1996	232			16	37
1998	290	81	123	23	47
1999	324				
2000	452				58

TABLE 3.  
PARAMETERS CHOSEN FOR THE CALCULATIONS IN FIGURE 3.

A <sub>f</sub>	Surface area of bent exposed to severe corrosion	20 m <sup>2</sup>
A <sub>e</sub>	Typical spall area	0.3 m <sup>2</sup>
C <sub>T</sub>	ECR chloride concentration threshold	1.55 kg/m <sup>3</sup>
C <sub>s</sub>	Average surface chloride concentration	14
s <sub>cs</sub>	Standard deviation of surface chloride concentration	C <sub>s</sub> /4
C <sub>smax</sub>	Maximum surface chloride concentration	14
x	Average rebar cover	76 mm
s <sub>cc</sub>	Standard deviation of rebar cover	x/4
D <sub>app</sub>	Average apparent chloride diffusion coefficient	2 · 10 <sup>-11</sup> m <sup>2</sup> /sec
s <sub>d</sub>	Standard deviation of app. diff. coeff.	D/4
k	Proportionality constant for propagation time (Percentages indicate fraction of the surface assigned to the value).	0.14 y/mm (2%); 0.28 y/mm (4%); 0.56 y/mm (8%).

Note: C<sub>s</sub>, x and D<sub>app</sub> were assumed to be distributed as in a standard deviation, but truncated by zero and as shown by C<sub>smax</sub>, and normalized accordingly.